

HOSTED BY

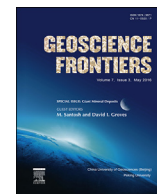


ELSEVIER

Contents lists available at ScienceDirect

China University of Geosciences (Beijing)

Geoscience Frontiers

journal homepage: [www.elsevier.com/locate/gsf](http://www.elsevier.com/locate/gsf)

Research paper

# The multistage genesis of the giant Dongshengmiao Zn-Pb-Cu deposit in western Inner Mongolia, China: Syngenetic stratabound mineralization and metamorphic remobilization

Richen Zhong<sup>a,b</sup>, Wenbo Li<sup>b,\*</sup><sup>a</sup> Civil and Environmental Engineering School, University of Science and Technology Beijing, Beijing 100083, China<sup>b</sup> Key Laboratory of Orogenic Belts and Crustal Evolution, School of Earth and Space Sciences, Peking University, Beijing 100871, China

## ARTICLE INFO

## Article history:

Received 26 June 2015

Received in revised form

12 September 2015

Accepted 20 September 2015

Available online 26 October 2015

## Keywords:

SEDEX

Zn-Pb-Cu

Metamorphism

Remobilization

Orogenic-type deposit

## ABSTRACT

The genesis of the giant Dongshengmiao in the northern margin of the North China Block has been debated since its discovery in the 1950s, because it shows geological and geochemical characteristics with both syngenetic and epigenetic signatures. It has geological settings and sulfur and lead isotopic compositions that are similar with typical SEDEX (sedimentary exhalative) deposit, while the Zn-Pb-Cu mineralization was controlled by shear deformation and metamorphism, showing similarities with orogenic-type deposits. In this contribution, both the syngenetic and epigenetic features of the Dongshengmiao are envisaged, and accounted for in the context of a genetic model with two metallogenic periods. Massive pyrite at the Dongshengmiao was mostly recrystallized during metamorphism, but fine-grained texture was locally preserved, indicating its syngenetic origin. On the contrary, all the Zn-Pb-Cu ores observed in this study show characteristics of epigenetic hydrothermal mineralization that controlled by metamorphism and accompanying shear deformation. The sulfur and lead isotopic compositions of sphalerite and galena indicate that they were *in situ* remobilized from a syngenetic stratabound source, and the oxygen and hydrogen isotopic ratios of ore-fluid indicate that the large-scale remobilization was assisted by metamorphic fluid. The thermodynamic modeling indicates that the ore-fluid during remobilization has a great potential of transporting Cu. This may account for the abnormally enriched Cu in the remobilized SEDEX deposit. The metamorphic fluid might strip Cu from the fluid source during devolatilization, and overprint it on the Zn-Pb orebodies during remobilization. A secondary flow-through modeling reveals that Zn- and Cu-sulfides would be preferentially redistributed in Fe-rich carbonates during remobilization, as a result of fluid-rock interaction. Conclusively, a multistage genetic model is proposed. During the development of the Proterozoic rift, stratabound Zn-Pb mineralization took place in a SEDEX ore-forming system. The syngenetic sulfides subsequently underwent a large-scale fluid-assisted remobilization during the early Cretaceous metamorphism and thrusting, forming the shear zone-controlled epigenetic orebodies. During the remobilization process, Cu was scavenged from the source of metamorphic fluid, and deposited accompanying remobilized Zn-Pb sulfides. Shear structures and Fe-rich carbonates are ideal sites for redistribution and re-deposition of remobilized sulfide.

© 2015, China University of Geosciences (Beijing) and Peking University. Production and hosting by Elsevier B.V. This is an open access article under the CC BY-NC-ND license (<http://creativecommons.org/licenses/by-nc-nd/4.0/>).

## 1. Introduction

The giant Dongshengmiao deposit has reserves of 4.83 Mt Zn at an average grade of 2.85% Zn, 0.96 Mt Pb at 0.67% Pb, and 0.11 Mt Cu at 0.86% Cu (Long, 2009), and is the third largest Pb-Zn deposit in

China following the Jinding and Changba-Lijiagou deposits (Wang et al., 2014). In addition, massive pyrite accompanying Zn-Pb-Cu mineralization is also mined for the purpose of making sulfuric acid. Since its discovery in the 1950s, the genesis of the Dongshengmiao deposit has been debated for more than half a century. Two end-member hypothesis of ore genesis have been proposed: (1) The submarine exhalative model stresses that syngenetic Zn-Pb-Cu mineralization was a result of submarine hydrothermal activity, and was slightly modified during subsequent metamorphism

\* Corresponding author.

E-mail address: [liwenbo@pku.edu.cn](mailto:liwenbo@pku.edu.cn) (W. Li).

Peer-review under responsibility of China University of Geosciences (Beijing).

and deformation (Xia, 1992; Jiang, 1994; Peng and Zhai, 2004; Peng et al., 2007a,b; Zhou et al., 2012; Gao et al., 2014). The authors proposed that the Dongshengmiao deposit shares similar geological settings with typical SEDEX deposits. For example, the ore-hosting rift sequences with interlayered siderite and B, Mn, P and Ba enriched layers are typical of SEDEX ore-forming systems (Yang, 1992; Peng et al., 2000; Peng and Zhai, 2004; Zhai et al., 2008). This model is also evidenced by geochemical features of sulfides, which is enriched in heavy S isotopes and depleted in radiogenic Pb isotopes (Miu and Ran, 1992). (2) An alternative epigenetic model stresses that the hydrothermal ore-forming process was structurally controlled during compressional deformation. This model is based on the observation that the distribution of sulfides was controlled by host rock deformation, especially by shear zone and folded strata (Niu et al., 1991; Sun and Niu, 1994).

The long-running debate between these competing models is mainly attributed to the paradoxical geological and geochemical features that show affinities with both syngenetic and epigenetic mineralization. For example, the orebodies are generally stratabound (e.g., Jiang, 1994; Zhou et al., 2012), but structural (e.g., Niu et al., 1991; Sun and Niu, 1994) and microscopic observations (Zhong et al., 2015b) indicate that sulfides were controlled by host rock deformation. Geochemical features of the deposit are also enigmatic. S and Pb isotopic ratios of sulfides are typical to SEDEX deposits, while H and O isotopes indicate a fluid source of metamorphic origin. Furthermore, although the Dongshengmiao has Zn and Pb tonnages and a Zn/(Zn + Pb) ratio similar to other SEDEX deposits all over the World, the unusual enrichment of Cu accompanying Zn and Pb is somehow atypical to most SEDEX deposits (Leach et al., 2005).

In recent years, the multistage genesis of the Dongshengmiao deposit is envisaged by some researchers, accounting for the hybrid syngenetic and epigenetic features of the deposit (Chen et al., 2009b). Based on the result of decrepitating temperatures of fluid inclusions, Peng et al. (2007a) proposed that magmatic fluid mineralization was responsible for the discordant Cu-Zn veinlets, which overprinted on stratabound orebodies. Zhang et al. (2010) envisaged the difference between massive pyrite and Zn-rich orebodies, and pointed out that the former is syngenetic while latter are results of epigenetic mineralization. Similarly, Gao et al. (2014) also noticed that Zn-rich orebodies are results of replacement mineralization when ore-fluid infiltrating dolomitic host rocks. Based on systematic microscopic observation and

$^{39}\text{Ar}/^{40}\text{Ar}$  geochronology, Zhong et al. (2015b) proposed that Zn-Pb-Cu sulfides are results of large-scale fluid-assisted remobilization of stratabound sulfides, during the early Cretaceous orogeny and accompanying thrusting and greenschist facies metamorphism.

The mixed syngenetic and epigenetic characteristics of the Dongshengmiao deposit are reviewed in this paper. These geological, geochemical and geochronological features together with our new petrographic observations are interpreted under the context of a multigenetic model. In addition, a thermodynamic modeling is carried out, accounting for the physicochemical process of remobilization as well as the atypical enrichment of Cu in the SEDEX deposit.

This case study may provide insights in understanding the geological and geochemical features and ore-forming processes of syngenetic base metal deposits (i.e., SEDEX and VMS deposits) that are hosted in metamorphic terranes. The gneisses of these deposits are commonly enigmatic and highly controversial, due to their complex ore-forming history involving synmetamorphic remobilization and/or hydrothermal overprinting (Marshall and Spry, 2000; Marignac et al., 2003; Gu et al., 2007; Moura, 2008; Xu et al., 2011; Zheng, 2013; Zheng et al., 2013; Brueckner et al., 2014). This study provides a quantitative constraint on metal budget during the multistage mineralization process.

## 2. Regional geological setting

The Dongshengmiao deposit is located in the Langshan district in the northern margin of the North China Block (NCB), bordered to the north by the Central Asian Orogenic Belt (CAOB) (Fig. 1). This Langshan area hosts three large (Huogeqi and Jiashengpan) and giant (Dongshengmiao) Cu-Pb-Zn polymetallic deposits and tens of medium-sized deposits (Fig. 2). The Archean basement of this area consists of high-grade metamorphosed basaltic and sedimentary rocks, and is overlain by greenschist to amphibolite facies Proterozoic rift rocks (Langshan Group). The latter, composed of mica schist, clastic metasedimentary rocks, carbonates, and intercalations of metavolcanic rocks (Peng et al., 2007b), are the immediate host rocks of all the Cu-Pb-Zn deposits in the Langshan area (Fig. 2). The Langshan Group was previously interpreted as Mesoproterozoic rift rocks, constrained by a whole rock Sm-Nd model age of  $1805 \pm 76$  Ma (Peng and Zhai, 1997). Based on a single U-Pb age of detrital zircon, Li et al. (2007) also reported a Mesoproterozoic depositional age of ca. 1750 Ma of the Zhaertai

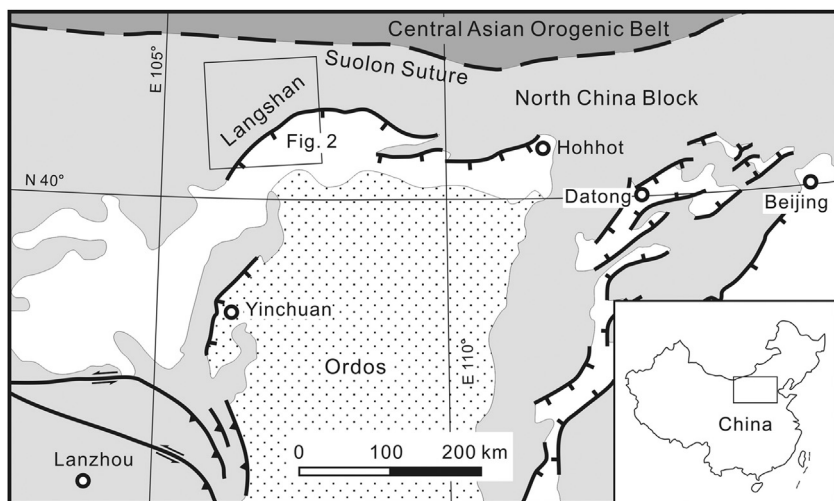


**Figure 1.** Location map of the northern China. Dark gray, Central Asian Orogenic Belt; light gray, North China Block; stippled pattern, Ordos Plateau (modified after Darby and Ritts, 2007).

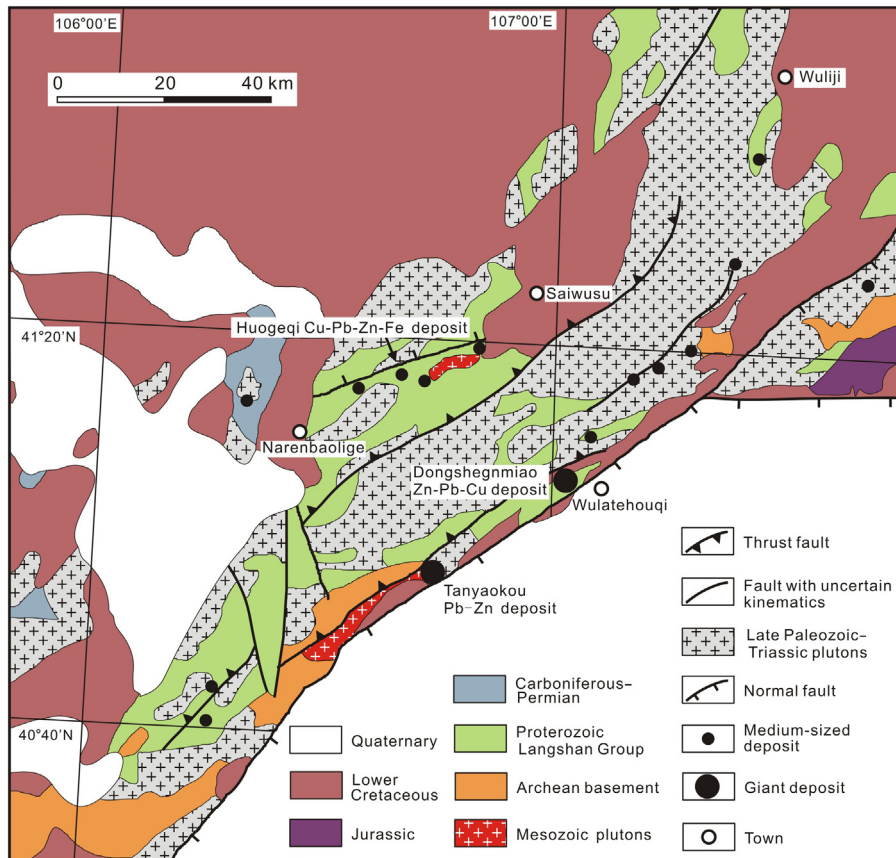


Figure 2. Regional geology of the Langshan district (modified after Peng et al., 2007b).

Group, which is regarded as the east continuation of the Langshan Group (Zhai et al., 2008). However, recent geochronological studies constrain its depositional age to be Neoproterozoic, constrained by dating of intercalated volcanic rocks with zircon U-Pb ages of  $867 \pm 10$  to  $805 \pm 5$  Ma (Peng et al., 2010) and  $804 \pm 3.5$  Ma (Gong, 2014). U-Pb dating of detrital zircons from metasedimentary rocks of the Langshan Group constrains them to be younger than 1100 Ma (Gong, 2014). It is still not clear whether there were more than one phases of rifting events, or the Langshan-Zhaertai Group is actually a collage of more than one terranes that of different affinities.

During Paleozoic times, the Paleo-Asian Ocean closed along the Suolon suture, leading to the development of the CAOB (Fig. 1). It is still a hot debate whether the Paleo-Asian Ocean finally closed in the Devonian (Xu et al., 2013) or in the late Permian–early Triassic (Sengör and Natal'in, 1996; Chen, 2002; Xiao et al., 2003; Chen et al., 2007a; Chen et al., 2009a; Zhang et al., 2009). Anyhow, late Paleozoic–Triassic biotite granite and granodiorite plutons are widely exposed in the Langshan area as a result of the prolonged orogenic event (Fig. 2).

At least ~100 million years after the continental collision between NCB and the Siberian Craton, a tectonic event took place in a large area of the central and eastern Asia during middle to late Mesozoic, also known as the Yanshanian movement in China (Yakubchuk, 2004; Dong et al., 2008). The geodynamic background of this tectonic event is still controversial and beyond this literature, but large-scale hydrothermal mineralization took place simultaneously, especially in eastern China (e.g., Chen et al., 2007a, 2012; Sun et al., 2007). The Langshan area is dominated by compressional deformation during this time, characterized by wide development of NE-trending thrust faults and contemporaneous deposition of red beds in foreland basins (Darby and Ritts, 2007).

### 3. Geology of the Dongshengmiao deposit

The Archean basement composed of gneiss and migmatite is exposed in the southeast of the Dongshengmiao deposit, and overlain by the ore-hosting Proterozoic Langshan Group (Figs. 2 and 3). Major lithological units of the lower greenschist facies Langshan Group include mica schist, carbonaceous shale, dolomitic marble and quartzite, with interlayered felsic and mafic metavolcanic rocks (Fig. 4). The protoliths of the Langshan Group are mainly sandstone, siltstone, mudstone and carbonates, which defines a coastal or shallow marine environment in a rift (Hebei College of Geology and Geological Prospecting Team of Inner Mongolia Chemical Industry, 1980). The Langshan Group is subdivided into three formations, termed as the First, the Second, and the Third Formation from the bottom to the top, respectively (Fig. 4). All the orebodies are hosted in the Second Formation, which is mainly composed of carbonaceous mica schist and dolomitic marble, with intercalated metavolcanic rocks at the bottom (Fig. 4). The Proterozoic ore-hosting rocks are overlain by the undeformed early Cretaceous terrestrial sediments, including red sandstone, conglomerate, and mudstone. These sediments are interpreted as molasses deposited in a foreland basin of an intra-plate orogeny (Darby and Ritts, 2007).

Northwest-dipping thrust faults and related mylonites are well developed in the Dongshengmiao deposit (Fig. 3). These thrusts are generally parallel to sedimentary beddings of the Proterozoic rocks (Suo, 1992), and consistently dip northwest at  $30^{\circ}$ – $45^{\circ}$  (Hu et al., 1981). Minimum displacements on the major thrusts are about 300 m (Hu et al., 1981). The age of thrusting is constrained as  $135.5 \pm 0.9$  Ma, by  $^{39}\text{Ar}/^{40}\text{Ar}$  dating of muscovite separated from shear deformed Proterozoic schist (Zhong et al., 2015b). These

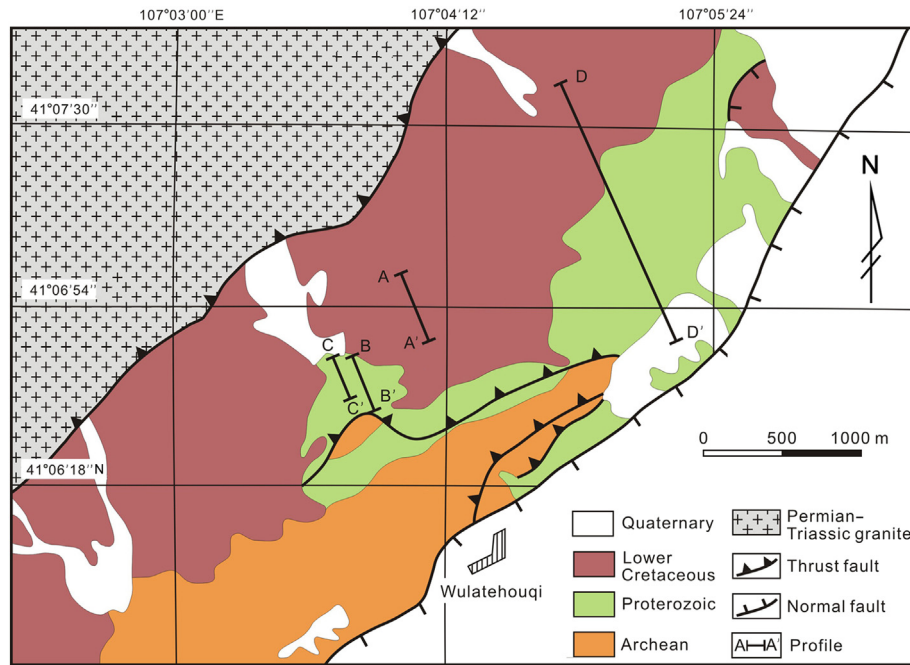


Figure 3. Geological map of the Dongshengmiao ore deposit (modified after Zhai et al., 2008).

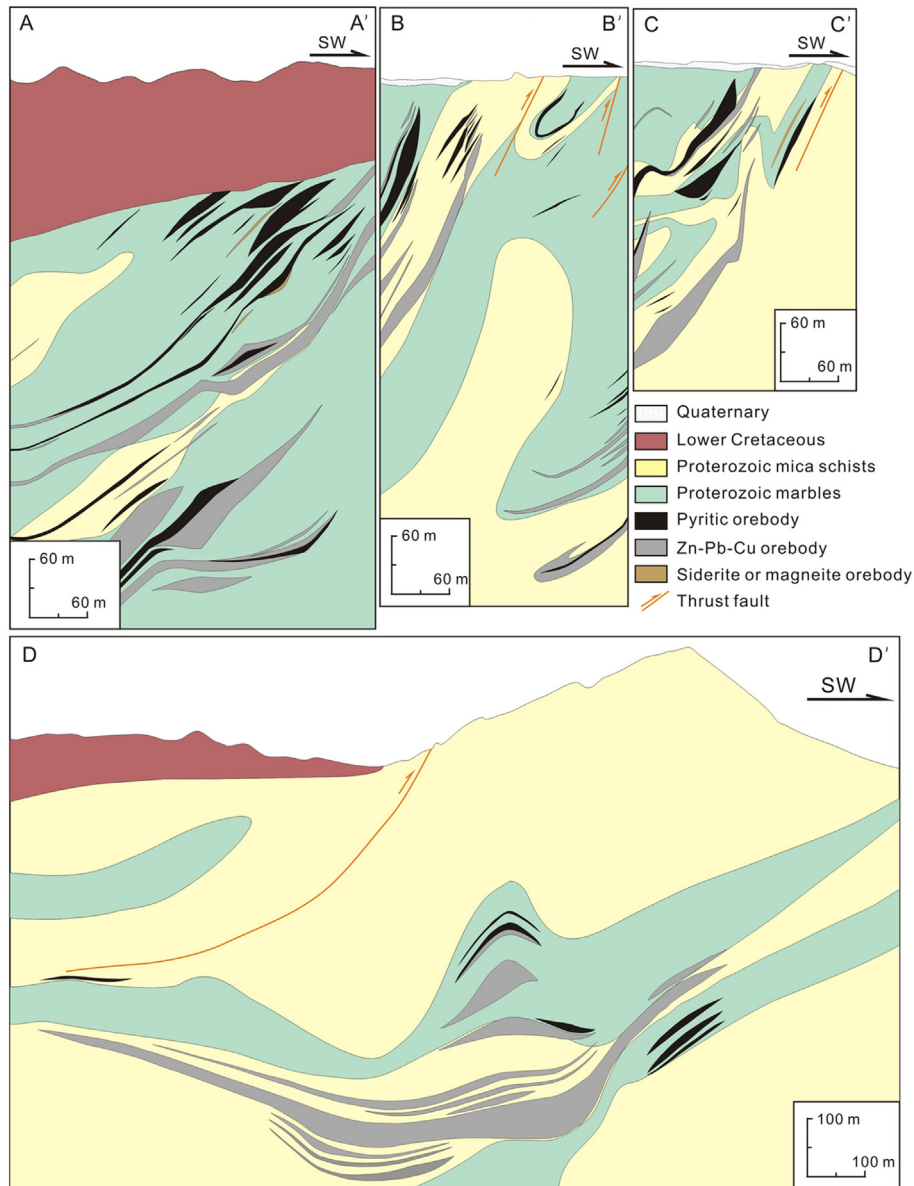
Strata	Thickness (m)	Stratigraphic Column	Lithology	Mineralization	
Lower Cretaceous	172		Red sandstone, conglomerate, and mudstone		
Proterozoic Langshan Group	Third Formation	150		Quartzite with interlayered mica schist	
		100		Chlorite muscovite schist	
	Second Formation	200		Carbonaceous schist with interlayered lime dolomite	
		200		Dolomite with interlayered carbonaceous schist and carbonaceous dolomite	Zn-Pb-Cu-S
		200		Carbonaceous schist with interlayered carbonaceous dolomite	Zn-Pb-Cu-S
	100		Dolomite with interlayered carbonaceous schist and metavolcanic rocks	S	
First Formation	315		Quartzite and two mica schist		
Archean	400		Gneiss and migmatite		

Figure 4. Stratigraphy of the ore-hosting Langshan Group at the Dongshengmiao deposit (modified after Rui et al., 1994 and Peng and Zhai, 1997).

thrusts were developed as a result of the intraplate orogeny and crustal shorting, coeval with the deposition of the early Cretaceous molasses (Darby and Ritts, 2007).

Permian–Triassic granitoids are widely exposed in the northwest of the deposit, separated from the early Cretaceous sediments by a thrust fault (Fig. 3). These plutons are composed of several phases of intrusive rocks emplaced from 287 to 228 Ma (Liu, 2012; Hu et al., 2015). Major lithological units include Permian quartz diorite and porphyritic granite (287–275 Ma; Hu et al., 2015), and Triassic monzogranite ( $245 \pm 5$  Ma; Liu, 2012) and granodiorite ( $228 \pm 4$  Ma; Liu, 2012). The tectonic setting of the Permian–Triassic magmatism is still controversial. The granitoids in the Dongshengmiao deposit are interpreted to be emplaced in a post-collisional setting (Hu et al., 2015), or as a result of the final closure of the Paleo-Asian Ocean (Liu, 2012).

The orebodies are mostly hosted in carbonaceous mica schist and dolomitic marbles of the Langshan Group, and overlain by the early Cretaceous molasses. Therefore they are not shown in Fig. 3. Orebodies are mostly northeast-trending and northwest-dipping, with dips of  $25^\circ$ – $65^\circ$  (Fig. 5; Wulatehouqi Zijin Mining Group Co. Ltd, 2008). The morphology of orebodies varies at different parts of the mining field. In the southwest region of the deposit (cross sections A–A', B–B' and C–C' in Fig. 3), where thrust faults are widely developed, the orebodies are steeply dipping and have high dip angles similar with the thrust faults (Fig. 5). They were asymmetrically folded as a result of thrusting (Fig. 5), and upgraded at hinge regions of the folds (Chen and Peng, 2008). Mineralization took place generally parallel to sedimentary beddings, but locally cut cross different lithological units (Fig. 5). In addition to Zn–Pb, most Cu mineralization occurs in the southwest region of the deposit. On the contrary, orebodies in the northeast segment (near the D–D' cross section in Fig. 3) of the deposit were relatively weakly deformed, and are generally stratiform and stratabound (Fig. 5), because thrust faulting was not as strong as that in the southwest (Fig. 3). The northeast region of the deposit is predominated by Zn–Pb and S mineralization, whereas Cu is generally subeconomic with an average grade of 0.08% Cu (Wulatehouqi Zijin Mining Group Co. Ltd, 2008). However, most orebodies in the



**Figure 5.** Cross section of orebodies of the Dongshengmiao deposit (modified after Wulatehouqi Zijin Mining Group Co. Ltd, 2008).

northeast region are enriched in silver, with an average grade of 11.9 g/t Ag (Wulatehouqi Zijin Mining Group Co. Ltd, 2008).

#### 4. Petrographic constraints

##### 4.1. Massive pyrite

Massive pyrite is common accompanying Zn-Pb-Cu mineralization (Fig. 6A–D), and it is mined as S ore for sulfuric acid. Most massive pyrite is coarse-grained ( $> \sim 100 \mu\text{m}$ ) due to metamorphic recrystallization (Fig. 6D and Fig. 6D in Zhong et al., 2015b), but fine-grained pyrite with typical grain sizes of  $\sim 10 \mu\text{m}$  is locally preserved (Fig. 6A, B). The fine-grained pyrite grains commonly have zoned textures, characterized by a dark yellow core surrounded by a clean rim (Fig. 6B). Some of the cores are relics of marcasite, manifested by their heterogeneity under polarizing microscopes, and the rims have been converted to pyrite during metamorphism. The darker color of the core indicates its greater

abundance of impurities compared to the recrystallized rim. Our unpublished results of *in situ* LA-ICP-MS analysis on sulfides indicate that the fine-grained massive pyrite is enriched in economic elements such as Zn and Pb.

Some massive pyrite was tectonically brecciated and cemented by hydrothermal minerals such as pyrite, pyrrhotite, Cu-Pb-Zn sulfides, and carbonates (Fig. 6A, C, D). Fine-grained pyrite was recrystallized with the assist of syn-tectonic fluid, especially adjacent to veinlets where channelized fluid infiltrating the massive pyrite (Fig. 6C). In cases that pervasive fluid infiltration took place along grain boundaries of pyrite, all the pyrite grains were recrystallized to grain sizes of  $> 100 \mu\text{m}$  (Fig. 6D).

##### 4.2. Zn-Pb-Cu mineralization

In deformed schist-hosted ores, Zn-Pb-Cu sulfides (sphalerite, galena, and chalcopyrite) are distributed in microstructures that formed during shear deformation of the host rocks. As shown in

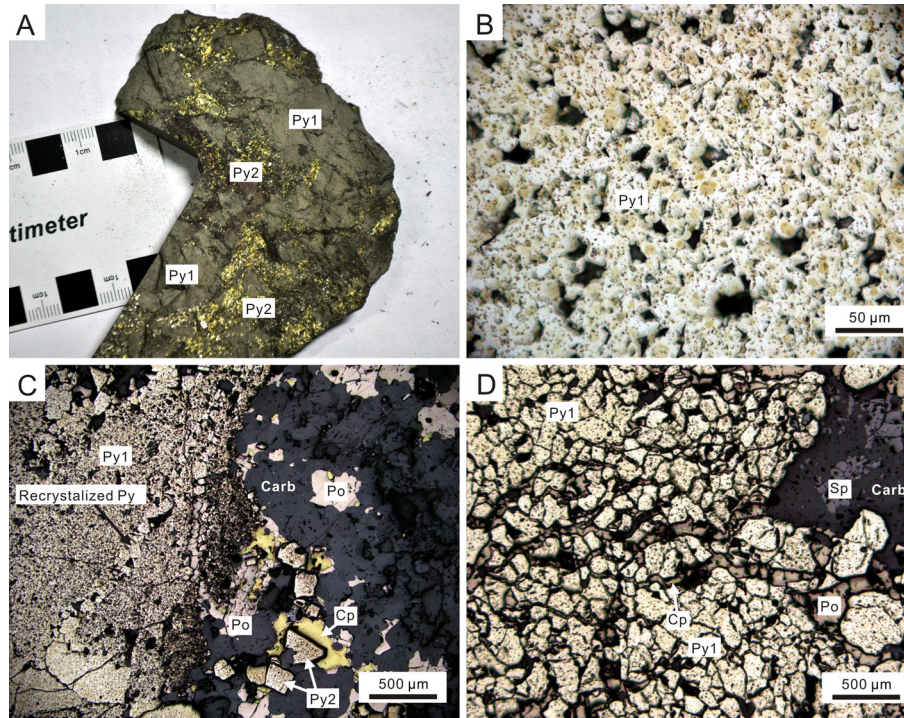


**Figure 6.** Petrographic characteristics of massive pyrite. Abbreviations: Py = pyrite; Py1 = syngenetic pyrite; Py2 = epigenetic hydrothermal pyrite; Po = pyrrhotite; Cp = chalcopyrite; Carb = carbonate; Sp = sphalerite. (A) Fine-grained massive pyrite was brecciated and cemented by coarse-grained hydrothermal pyrite (hand specimen). (B) Fine-grained syngenetic pyrite (reflected light). (C) Fine-grained massive pyrite was infiltrated by hydrothermal solution along microfractures, and recrystallized near the fractures (reflected light). (D) Massive pyrite was recrystallized when pervasive fluid infiltrating along grain boundaries (reflected light).

Fig. 7A, B, the ore-hosting carbonaceous schist is tectonically brecciated under shear stress, forming discrete, oriented, and asymmetric rhombic fragments. Sulfide-bearing veinlet developed parallel to the shear band (i.e., C foliations of mylonite; Fig. 7A, B). In the veinlet, syn-ore hydrothermal gangue minerals such as muscovite and quartz are oriented parallel to the S foliations of the mylonitic host rock (Fig. 7A, B). This indicates that the ore-bearing fluid was introduced during shear deformation of the host rock.

High-grade Zn-Pb ores are mostly hosted in the chemically active Fe-rich marble, which is mainly composed of siderite-magnesite (Fig. 7C–E). Sulfides are distributed along grain boundaries of the carbonate host rocks, locally corroding and replacing host carbonates (Fig. 7C–E). Biotite was commonly generated at contact between sulfides and Fe-Mg carbonates (Fig. 7E). Zn-Pb mineralization hosted in Fe-rich carbonate is commonly accompanied by precipitation of large amounts of pyrrhotite or pyrrhotite-pyrite ± magnetite assemblage (Fig. 7E).

Some high-grade Zn-Pb mineralizations are the ‘breccia-type ore’ defined by previous researchers (e.g., Peng et al., 2000). The breccia elements of this type of mineralization are fragments of foliated ore-hosting marble and mica schist, and the matrix are composed of fine-grained Fe-rich carbonates (Fig. 7C, D). The foliations of host rock fragments are inconsistently orientated in different fragments (Fig. 7C, D). Zn-Pb-Cu sulfides in the breccia-type ores occur along grain boundaries of fine-grained carbonates in the matrix and cement host rock fragments (Fig. 7C, D).

Accompanying the precipitation of Zn-Pb-Cu sulfides, pyrite, pyrrhotite, biotite, muscovite, chlorite, carbonates and quartz are common hydrothermal gangue minerals observed in most ores (Fig. 7B, F–H), defining an ore-forming P-T condition consistent with lower greenschist facies metamorphism. Besides, barite is also observed accompanying sulfides, and witherite was generated at

contact between barite and carbonate host rocks. Magnetite was mostly formed during the earliest stage of sulfide precipitation, it commonly occurs at contacts between hydrothermal veinlets (channelized fluid pathway) and host rocks, accompanying pyrite and pyrrhotite (Fig. 7G, H). In areas where the fluid infiltrating into the host rocks and centimeters away from the veinlets, magnetite is absent and the Fe-S-O mineral assemblage is characterized by pyrite-pyrrhotite or pyrrhotite-only.

#### 4.3. Interpretations

Although most massive pyrite at the Dongshengmiao was recrystallized during subsequent metamorphism and fluid infiltration (Fig. 6D), fine-grained texture is still preserved in some samples (Fig. 6A–C), which is an index of syngenetic mineralization (Leach et al., 2005). Additionally, the relics of marcasite as cores in the fine-grained pyrite crystal also manifest the low-temperature syngenetic origin of massive pyrite.

Syngenetic massive pyrite was tectonically brecciated and cemented by coarse-grained sulfides and accompanying hydrothermal gangue minerals (Fig. 6A), or infiltrated by hydrothermal fluid along grain boundaries or microfractures (Fig. 6C, D), indicating an overprinting of hydrothermal ore-fluid on the syngenetic massive pyrite. All the chalcopyrite, galena and sphalerite that observed in this study were formed during this hydrothermal event. In strongly sheared host rocks, sulfides and accompanying gangue minerals such as quartz, muscovite, and carbonate precipitated filling shear structures (e.g., S-C foliations; Fig. 7A, B), indicating that hydrothermal mineralization was coeval with shear deformation of the host rocks.

By comparing between the mineralization styles and Fe-contents of host rocks, Zhong et al. (2015b) proposed that Fe-rich

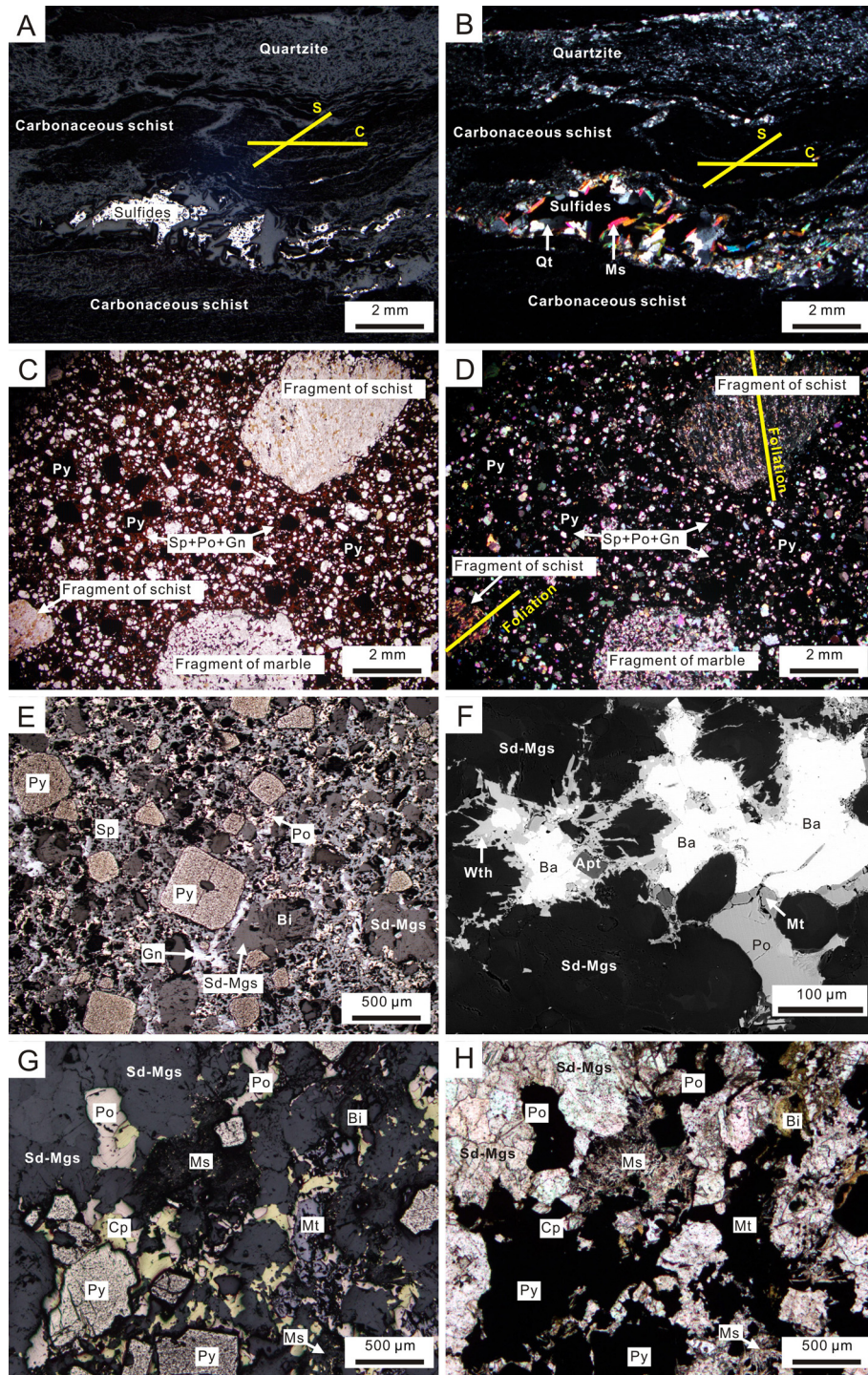


**Figure 7.** Petrographic characteristics of Zn-Pb-Cu mineralization. Abbreviations: Qt = quartz; Ms = muscovite; Gn = galena; Sd-Mgs = siderite-magnesite; Ba = barite; Wth = witherite; Mt = magnetite; Bi = biotite. Other abbreviations are as in Fig. 6. (A) Sulfide-bearing veinlets were developed parallel to shear bands (C foliation) of mylonitized carbonaceous schist, and accompanying hydrothermal quartz and muscovite oriented parallel to S foliations of the mylonite (reflected light). (B) The same field of view as (A), but in plane-polarized light. (C) “Breccia-type” mineralization. Fragments of foliated host rocks are cemented by Zn-Pb sulfides. The matrix is composed of fine-grained Fe-Mg carbonates and was infiltrated by the ore-fluid along grain boundaries. Note that the host rock fragments are inconsistently orientated (plane-polarized light). (D) The same field of view as (C), but in crossed polars. (E) Sulfides distribute along grain boundaries of siderite-magnesite, and eroded and replaced the ore-hosting siderite-magnesite. Biotite was generated at contacts between sulfides and Fe-Mg carbonates (reflected light). (F) Barite precipitated accompanying sulfides and magnetite, and witherite was generated at contacts between barite and ore-hosting siderite-magnesite (backscatter electron image). (G) The coexistent magnetite, pyrite, and pyrrhotite in a Fe-Mg carbonate-hosted ore (reflected light). (H) The same field of view as (G), but in plane-polarized light.

carbonates are ideal sites for high-grade mineralization (Fig. 7C, D). Fe-rich carbonates are chemically active and therefore favored precipitation of sulfides. Host rock carbonates were eroded by the ore-fluid during fluid infiltration along grain boundaries,

manifested by the rounded and embayed relics of carbonates (Fig. 7E). A skarn-like fluid-rock interaction is indicated by the formation of biotite at contact between ore-fluid and Fe-Mg carbonates (Fig. 7E and Fig. 8A, F in Zhong et al., 2015b).

Compared with strongly deformed metamorphic minerals of the host rock, sulfides and accompanying hydrothermal gangue minerals are generally strain-free or weakly deformed (Fig. 7), indicating that hydrothermal mineralization took place at the latest stage of shear deformation. This also excludes the possibility that the high-grade replacement mineralization took place during the diagenetic process of the ore-hosting carbonates (e.g., Leach et al., 2010). Particularly, in the breccia-type ores, the inconsistently orientated foliations of different breccia elements (Fig. 7C, D) indicate that the brecciating of host rocks postdated their metamorphism and foliating, and the previously foliated host rock fragments were rotated during brecciation. The host rocks were brecciated under shear stress, and the fine-grained matrix cementing the fragments are tectonically milled host rocks during shear deformation, i.e., cataclastic rocks of a shear zone. The 'breccia-type' Zn-Pb-Cu mineralization took place when the syntectonic ore-fluid infiltrating the matrix of cataclastically deformed carbonate.

The pressure-temperature (P-T) condition of Zn-Pb-Cu mineralization is constrained by the assemblage of hydrothermal gangue minerals accompanying sulfides, which mainly include muscovite, biotite, chlorite, quartz and carbonates (Figs. 6C, D and 7B, E, G, H). This indicates a lower greenschist facies P-T condition during mineralization. Previous fluid inclusion study shows that total homogenization temperatures of inclusions in mineralized quartz veins cluster at 300–380 °C with a mode at 340–360 °C (Miu and Ran, 1992), consistent with the lower greenschist facies temperatures. In our previous work, an ore-forming depth of ~7–10 km is determined using sphalerite geobarometer (Zhong et al., 2015b), which is also a crustal depth of lower greenschist facies regime. Taken that the lower greenschist facies host rocks, represented by chlorite muscovite schist and two-mica schist, have similar metamorphic mineral assemblage with Zn-Pb-Cu ores, the mineralization took place simultaneously with host rock metamorphism.

Conclusively, two periods of metallogenesis are recognized based on petrographic observation: syngenetic massive pyrite overprinted by syntectonic and synmetamorphic Zn-Pb-Cu hydrothermal mineralization. Although Zn and Pb were deposited from an epigenetic fluid, isotopic signatures indicate that they were remobilized from syngenetic stratabound sulfides (see the following section). Samples observed in this study were collected from the southwest segment of the deposit, where the thrust-related shear deformation was intensive. Therefore, seldom syngenetic Zn-Pb-Cu sulfides were preserved there due to the pervasive fluid-assisted remobilization accompanying shear deformation. It is highly probable that some syngenetic stratabound Zn-Pb orebodies were preserved at the Dongshengmiao deposit (especially in the northeast segment), although they were not observed in this study. Our unpublished *in situ* LA-ICP-MS analysis on sulfides revealed that the syngenetic massive pyrite/marcasite has high concentrations of impurities such as Zn and Pb, indicating that Zn-Pb pre-enrichment took place during the syngenetic process.

## 5. Isotopic constraints

In this section, the results of previously published lead, sulfur, oxygen, and hydrogen isotopic researches are compiled, in order to trace the sources of S, Pb and ore-fluid, and to reveal the ore-forming history of the Dongshengmiao deposit.

### 5.1. Lead isotopes of sulfides

Lead isotopic ratios of galena, sphalerite, pyrite, and pyrrhotite were reported by Li et al. (1986), Ding and Jiang (2000), and Huang (2009) (Table 1). All the sulfide minerals at Dongshengmiao are

typically depleted in radiogenic lead, with two-stage model ages of ca. 2000 to 1750 Ma (Fig. 8).

### 5.2. Sulfur isotope of sulfides

We compiled the sulfur isotope ratios of sulfides that published in previous literature (Chen, 1990; Miu and Ran, 1992; Ding and Jiang, 2000). All sulfides except for chalcopyrite are characterized by enrichment in heavy sulfur isotope with  $\delta^{34}\text{S}$  values higher than 13‰ (Table 2, Fig. 9). Pyrite in the Dongshengmiao mostly occurs as recrystallized massive pyrite that formed during the submarine exhalative process, and has an average  $\delta^{34}\text{S}$  value of  $27.5 \pm 7.2$ ‰ (1 $\sigma$ ,  $n = 24$ ). Pyrrhotite, sphalerite, and galena were precipitated from an epigenetic hydrothermal solution during metamorphism and shear deformation, and they have a  $\delta^{34}\text{S}$  value of  $23.7 \pm 6.3$ ‰ in average (1 $\sigma$ ,  $n = 45$ ). The sulfur isotope of chalcopyrite is distinctly lighter than other sulfides (Fig. 9), with an average  $\delta^{34}\text{S}$  value of  $2.5 \pm 2.5$ ‰ (1 $\sigma$ ,  $n = 4$ ).

### 5.3. Oxygen and hydrogen isotopes of ore-fluid during Zn-Pb-Cu mineralization

Ding and Jiang (2000) reported the oxygen isotopic compositions of ore-forming fluids during epigenetic Zn-Pb-Cu mineralization, based on direct measurement of oxygen isotopes of syn-ore hydrothermal quartz ( $\delta^{18}\text{O} = 17.9\text{--}18.0$ ‰) and biotite ( $\delta^{18}\text{O} = 9.0\text{--}12.7$ ‰). Hydrogen isotopic ratio of hydrothermal biotite ( $\delta\text{D} = -95$  to  $-134$ ‰) and fluid inclusion water ( $\delta\text{D} = -60$  to  $-83$ ‰) extracted from hydrothermal quartz are also reported, to reveal the  $\delta\text{D}$  values of ore-fluid (Ding and Jiang, 2000; Table 3). The  $\delta^{18}\text{O}$  values of ore-fluid are calculated using the biotite–water fractionation equation from Zheng (1993) and quartz–water by Clayton et al. (1972), assuming mineral precipitation at 350 °C. The  $\delta\text{D}$  values are calculated in equilibrium with biotite based on the extrapolation of biotite–water fractionation equation by Suzuoki and Epstein (1976) at 350 °C. Based on the calculations and direct hydrogen isotopic measurement of fluid inclusion water,  $\delta\text{D}$  and  $\delta^{18}\text{O}$  values of ore-fluids range from  $-83$  to  $-37$ ‰ and 10.7 to 14.4‰, respectively (Table 3, Fig. 10).

**Table 1**  
Lead isotopic ratios of sulfides.

Mineral	$^{206}\text{Pb}/^{204}\text{Pb}$	$^{207}\text{Pb}/^{204}\text{Pb}$	$^{208}\text{Pb}/^{204}\text{Pb}$	Sources
Galena	15.2203	14.9812	35.1643	Huang (2009) and references therein
Galena	15.1061	15.0531	36.1538	
Galena	15.1350	14.9440	35.3230	Li et al., 1986
Galena	15.2860	15.1310	35.2950	
Galena	15.2200	14.9810	35.1640	
Galena	15.1060	15.0530	35.1540	
Pyrite	15.0886	15.0642	34.9849	
Pyrite	15.2246	15.3543	35.2667	
Pyrite	15.5510	15.1250	35.4830	
Pyrrhotite	15.1707	15.0849	35.1460	
Galena	15.6560	15.1780	36.6820	
Galena	15.4150	15.1450	35.2530	
Galena	15.1900	14.9100	35.3000	
Galena	14.7800	14.5000	35.0100	
Sphalerite	16.3010	15.3200	36.1940	
Sphalerite	16.3210	15.3200	36.1140	
Sphalerite	15.7320	15.2210	35.7710	
Sphalerite	15.7280	15.2340	35.8260	
Sphalerite	15.3350	15.1510	35.4000	
Sphalerite	15.7320	15.2210	35.7710	
Sphalerite	15.7420	15.2020	35.7590	
Pyrite	15.2020	15.1440	35.2810	Ding and Jiang, 2000
Pyrite	15.1710	15.1820	35.4350	

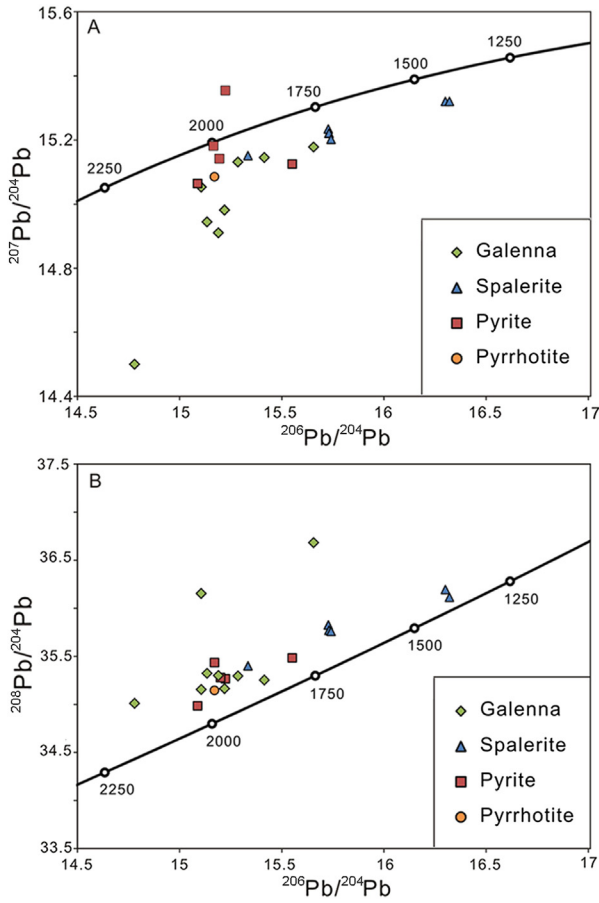


**Figure 8.** Lead isotope data on sulfides. The two-stage lead growth curve is from Stacey and Kramers (1975). The numbers along the growth curve are two-stage lead model ages, in millions of years. The lead isotope data of sulfides are compiled from Li et al. (1986), Ding and Jiang (2000) and Huang (2009). (A)  $^{206}\text{Pb}/^{204}\text{Pb}$ – $^{207}\text{Pb}/^{204}\text{Pb}$  diagram. (B)  $^{206}\text{Pb}/^{204}\text{Pb}$ – $^{208}\text{Pb}/^{204}\text{Pb}$  diagram.

5.4. Interpretation

As discussed above, Zn-Pb-Cu mineralization at the Dongshengmiao was controlled by shear deformation during greenschist facies metamorphism. Our previous  $^{39}\text{Ar}/^{40}\text{Ar}$  geochronological study revealed that Zn-Pb-Cu mineralization took place in the early Cretaceous ( $135.6 \pm 0.8$  Ma), coeval with host rock metamorphism and shear deformation ( $135.5 \pm 0.9$  Ma) (Zhong et al., 2015b). However, lead isotopes of sulfides are significantly depleted in radiogenic lead compared with the age of sulfide precipitation. Sulfides mostly have two-stage lead model ages of ~2000–1750 Ma (Fig. 8), whereas their precipitation took place in early Cretaceous (~136 Ma). This indicates that the early Cretaceous ore-bearing fluid was derived from an extremely lead-enriched source, which has a much lower U/Pb (and Th/Pb) ratio than average crustal rocks. Based on the two-stage lead model ages, the lead enrichment process might take place during Proterozoic, coeval with deposition of the ore-hosting Langshan Group. Conclusively, during the epigenetic Zn-Pb-Cu mineralization, lead was remobilized from stratabound orebodies that were syngenetically formed during the deposition of the Proterozoic Langshan Group.

The syngenetic pre-enrichment process is also verified by the sulfur isotopic signatures of sulfides, which are significantly enriched in heavy sulfur isotopes, except for chalcopyrite (Fig. 9). The enrichment of heavy sulfur isotopes is diagnostic of submarine

**Table 2**  
Sulfur isotopic ratios of sulfides.

$\delta^{34}\text{S}$ (‰)					Sources
Pyrite	Pyrrhotite	Sphalerite	Galena	Chalcopyrite	
16.5 <sup>a</sup>	16.5 <sup>a</sup>	13.5 <sup>a</sup>	27.5 <sup>a</sup>	-0.5 <sup>a</sup>	Chen, 1990 <sup>a</sup>
20.5 <sup>a</sup>	16.5 <sup>a</sup>	15.5 <sup>a</sup>		2.5 <sup>a</sup>	
20.5 <sup>a</sup>	16.5 <sup>a</sup>	18.5 <sup>a</sup>			
20.5 <sup>a</sup>	16.5 <sup>a</sup>	24.5 <sup>a</sup>			
21.5 <sup>a</sup>	18.5 <sup>a</sup>	24.5 <sup>a</sup>			
29.5 <sup>a</sup>	21.5 <sup>a</sup>	29.5 <sup>a</sup>			
31.5 <sup>a</sup>	21.5 <sup>a</sup>				
31.5 <sup>a</sup>	22.5 <sup>a</sup>				
32.5 <sup>a</sup>	22.5 <sup>a</sup>				
32.5 <sup>a</sup>	26.5 <sup>a</sup>				
35.5 <sup>a</sup>	32.5 <sup>a</sup>				
40.5 <sup>a</sup>	35.5 <sup>a</sup>				
41.5 <sup>a</sup>	40.5 <sup>a</sup>				
41.5 <sup>a</sup>	41.5 <sup>a</sup>				
23.0	23.9	21.7	22.6	2.1	Miu and Ran, 1992
23.5	29.1	27.7	30.1	5.7	
22.9	23.9	19.2			
22.9	24.3	17.1			
23.1	19.5	21.1			
19.5	19.2				
	20.2				
	19.2				
	19.3				
	21.5				
37.0	23.9	28.6	22.6		Ding and Jiang, 2000
30.4	29.1	34.6			
35.8		21.7			
23.5		21.7			
23.0					

<sup>a</sup> The raw data are now presented by the author, and therefore the  $\delta^{34}\text{S}$  values are deduced from the histogram of  $\delta^{34}\text{S}$  values (Fig. 3 in Chen, 1990). For example, if the histogram shows a  $\delta^{34}\text{S}$  value between 16 and 17‰, it is presented as 16.5‰ in this table.

exhalative deposits such as SEDEX, the sulfur of which are mainly derived from non-bacterial reduction of isotopically heavy marine sulfate (Ohmoto and Rye, 1979). Most pyrite at the Dongshengmiao is from recrystallized massive pyrite, and therefore its isotopic composition ( $\delta^{34}\text{S} = 27.5 \pm 7.2$ ‰) in average) represents the syngenetic stratabound sulfides. The average  $\delta^{34}\text{S}$  value of epigenetic hydrothermal pyrrhotite, galena, and sphalerite is  $23.7 \pm 6.3$ ‰. Since the fractionation factor between aqueous  $\text{H}_2\text{S}$  and solid sulfides is lower than 1‰ (Ohmoto and Rye, 1979), this value represents the isotopic composition of reduced sulfur in the ore-fluid. Due to the presence of sulfate in the hydrothermal solution, which is manifested by the presence of barite (Fig. 7F), the fractionation between aqueous  $\text{H}_2\text{S}$  (and  $\text{HS}^-$ ) and the bulk dissolved sulfur is not negligible. The factor of fractionation depends on the  $\sum \text{SO}_4^{2-} / \sum \text{H}_2\text{S}$  ratio and fluid temperature (Ohmoto and Rye,

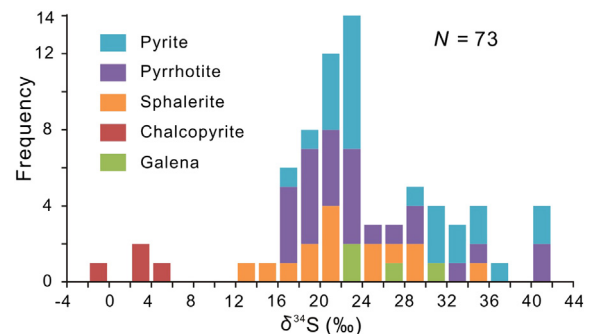


**Figure 9.** Histogram of  $\delta^{34}\text{S}$  values of sulfides. The sulfur isotope data of sulfides are compiled from Chen (1990), Miu and Ran (1992), and Ding and Jiang (2000).

**Table 3**  
Hydrogen and oxygen isotopic ratios of the Dongshengmiao deposit.

Sample type	Analyzed mineral	$\delta^{18}\text{O}$ (‰)		$\delta\text{D}$ (‰)	
		Mineral	Water	Mineral	Water
Pyrite-bearing quartz vein	Biotite	11.5	13.2	-112	-54
Pyrite-bearing quartz vein	Biotite	12.7	14.4	-130	-72
Pyrite-bearing quartz vein	Biotite	9.0	10.7	-134	-76
Pyrite-bearing quartz vein	Biotite	12.0	13.5	-95	-37
Pyrite-bearing quartz vein	Biotite	12.7	14.2	-106	-48
Pyrrhotite-rich ore	Quartz	17.9	12.1	–	-83
Pyrite-bearing quartz vein	Quartz	18.0	12.2	–	-60
Mineralized quartz vein	Quartz	17.9	12.1	–	-80

1979). Thermodynamic modeling (see below) reveals that there is near equal aqueous sulfate and reduced sulfur in the fluid at 350 °C ( $\Sigma\text{SO}_4^{2-}/\Sigma\text{H}_2\text{S} = \sim 1.7$ ; Fig. 11). This indicates that the bulk fluid sulfur would be heavier than the equilibrated sulfides by a factor  $\sim 5\text{--}10\%$  (Ohmoto and Rye, 1979). The sulfur isotope of syngenetic pyrite is  $\sim 4\%$  heavier than that of epigenetic hydrothermal sulfides, consistent well with the hypothesis that the epigenetic Zn-Pb sulfides was remobilized from stratabound sulfides.

Sulfur isotopic composition of chalcopyrite is distinctly different from sphalerite and galena, and its  $\delta^{34}\text{S}$  value is significantly lower than sphalerite and galena by more than 20‰ (Fig. 9). Such a great difference can not be accounted for by isotopic fractionation, for the fractionation factor between chalcopyrite and aqueous  $\text{H}_2\text{S}$  is as low as  $-0.1\%$  at 350 °C (Ohmoto and Rye, 1979). Furthermore, chalcopyrite precipitated generally coeval with other sulfides, and therefore their great difference in sulfur isotopes can not be an effect of Rayleigh fractionation. The distinct isotopic signature of chalcopyrite indicates that the Cu-mineralized fluid might be derived from a different source rather than the stratabound Zn and Pb. This possibility will be further discussed in the following sections.

The source of ore-fluid during Zn-Pb-Cu mineralization is traced by hydrogen and oxygen isotopes of ore-fluid. The ore-forming fluid is characterized by enrichment of heavy oxygen isotope, which is identical to pelitic metamorphic fluid (Fig. 10; Goldfarb et al., 1991). Hydrogen of the ore-fluid is generally isotopically heavy, with about half of the data plotted within the regime of

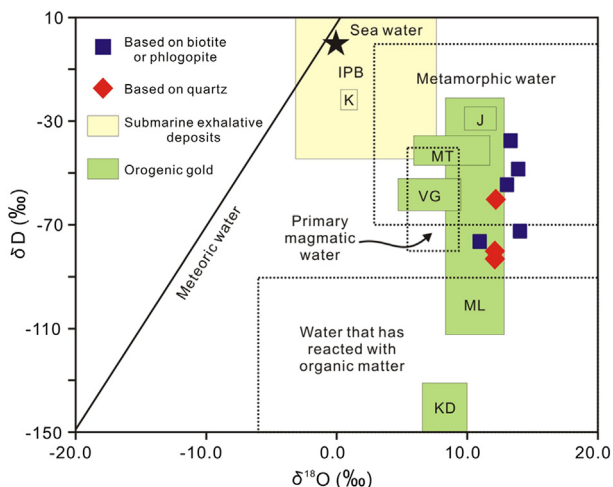


**Figure 10.** Plots of  $\delta^{18}\text{O}$  versus  $\delta\text{D}$  for the ore-fluid during sulfide remobilization. The H-O isotopes of orogenic gold deposits are after Goldfarb et al. (2005); and the submarine exhalative deposits are from Ohmoto and Rye (1979); Kuroko) and Tornos (2006; Iberian Pyrite Belt). The isotopic composition of natural waters with different origins is after Taylor (1974) and Sheppard (1986). Abbreviations: J = Juneau; MT = Meguma Terrane; VG = Victorian Goldfields; ML = Mother Lode; KD = Klondike; K = Kuroko; IPB = Iberian Pyrite Belt.

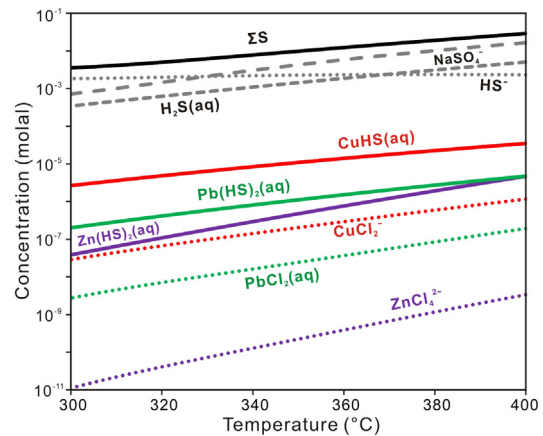


**Figure 11.** The result of thermodynamic modeling on the initial ore-fluid during hydrothermal remobilization, showing the solubility of major aqueous S-, Zn-, Pb-, and Cu-species in a hydrothermal solution with 1 molal NaCl and saturated with chalcopyrite, galena, sphalerite, pyrite, magnetite, pyrrhotite, barite, dolomite, muscovite, quartz, and biotite. The modeling is carried out at 2.5 kbar.

metamorphic fluid, but showing a trend towards the regime of water that interacted with organic matters (Fig. 10). This indicates that the ore-fluid might be derived from devolatilization of pelitic rocks during metamorphism and interacted with carbonaceous shale during fluid migration. This hypothesis is consistent with the fact that carbonaceous schist and marble are common in the host rock sequences (Fig. 4). Ore-fluid of the Dongshengmiao is mesothermal and enriched in  $\text{CO}_2$  and  $\text{N}_2$  (Miu and Ran, 1992), which are also characteristics of metamorphic fluids (Goldfarb et al., 2005; Chen et al., 2007b).

The hydrogen and oxygen isotopic ratios of ore-fluid at the Dongshengmiao are similar with orogenic gold deposits (Fig. 10), which are typical cases of shear zone controlled metamorphic fluid deposits (Goldfarb et al., 2005; Chen, 2006). However, they are significantly different from typical submarine exhalative deposits (Fig. 10), which are mainly formed from modified sea water with  $\delta\text{D}$  and  $\delta^{18}\text{O}$  values close to 0‰ (Fig. 10). This indicates a large-scale remobilization assisted with metamorphic fluid, which totally modified the oxygen and hydrogen isotopic signatures of the syngenetic orebodies (Marshall and Spry, 2000).

## 6. Thermodynamic modeling of Zn-Pb-Cu mineralization

Two runs of thermodynamic modeling are carried out using the HCh package and the updated Unitherm database (Shvarov and Bastrakov, 1999). Detailed descriptions on the methodology and selections of thermodynamic properties of minerals and aqueous species are provided by Zhong et al. (2015a). In the first run of modeling, we modeled Zn, Pb, Cu, and S speciation and solubility in the initial ore-fluid during Zn-Pb-Cu mineralization (hydrothermal remobilization), to reveal the physicochemical conditions and metal speciation of the fluid. In the second run of modeling, the ore-fluid flows through different lithological units that simulate the host rock sequences, to reveal lithological controls on metal precipitation.

### 6.1. The initial ore-fluid

Magnetite mostly occurs near contacts between the hydrothermal veinlets and host rocks, suggesting that it precipitated early during fluid evolution. In some cases, magnetite precipitated together with both pyrite and pyrrhotite (Fig. 7G), which defines the  $a_{\text{H}_2\text{S}}\text{-}f_{\text{O}_2}$  condition of the fluid near the magnetite-pyrite-

pyrrhotite triple junction of the Fe-S-O-H system (e.g., see Fig. 12 in Zhong et al., 2012). Although the magnetite-pyrite-pyrrhotite assemblage does not occur in all the Zn-Pb-Cu ores, it provides a good constraint on the  $a_{\text{H}_2\text{S}}-f_{\text{O}_2}$  condition of the initial ore-fluid. The presence of syn-ore barite (Fig. 7G) provides another constraint on speciation of sulfur in the ore-forming fluid. Other syn-ore hydrothermal minerals mainly include dolomite, quartz, muscovite, and biotite (Figs. 6C, D and 7B, E, G, H). These minerals constrain the ore-fluid to be  $\text{CO}_2$ -rich and have near-neutral pH. The fluid salinity has not been precisely analyzed, for previous fluid inclusion studies were carried out using only heating stages and can only measure the high-salinity inclusions with daughter minerals (e.g., Miu and Ran, 1992). Our preliminary petrographic observation on fluid inclusion reveals that most inclusions at the Dongshengmiao are carbon-rich and without daughter minerals, similar with those of typical orogenic gold deposits (Goldfarb et al., 2005). Therefore we arbitrarily set the fluid salinity as 1 molal NaCl (~5.5 wt.% NaCl), typical to orogenic-type deposits. To test the influence of fluid salinity on metal speciation, a secondary simulation of 5 molal NaCl (~23 wt.% NaCl) was carried out, and the simulated results are not significantly changed (not shown). The greatest uncertainty of the simulation is the fluid temperature, which will influence equilibrium of reactions. The simulation is carried out over a temperature range of 300–400 °C, which covers the whole range of estimated ore-forming temperatures. The pressure is fixed at 2.5 kbar, based on results of sphalerite geobarometer (Zhong et al., 2015b). Therefore, in the Zn-Pb-Cu-Fe-Mg-Ca-Ba-Na-K-Al-Si-S-C-Cl-O-H system, we simulated the equilibrium between a solution with 1 molal NaCl and solid phases including chalcopyrite, galena, sphalerite, pyrite, magnetite, pyrrhotite, barite, dolomite, muscovite, quartz, and biotite, over the temperature range of 300–400 °C at 2.5 kbar.

The simulated Zn, Pb, Cu and S solubility and speciation are shown as functions of fluid temperature (Fig. 11). Due to

equilibrium with both barite and Fe-S minerals, the ore-fluid is enriched in sulfur (0.004–0.03 molal), and has near-equal concentrations of sulfate (mainly  $\text{NaSO}_4^-$ ) and reduced sulfur (mainly  $\text{H}_2\text{S}(\text{aq})$  and  $\text{HS}^-$ ) (Fig. 11). The predicted concentration of reduced sulfur is consistent with the typical orogenic gold-forming fluids that containing  $10^{-3}$ – $10^{-0.5}$  molal reduced sulfur (Goldfarb et al., 2005). Zn, Pb, and Cu in the ore-fluid are predominated by electrically neutral hydrosulfide complexes ( $\text{Zn}(\text{HS})_2(\text{aq})$ ,  $\text{Pb}(\text{HS})_2(\text{aq})$ , and  $\text{CuHS}(\text{aq})$ ; Fig. 11), consistent with the theoretical prediction that Zn-, Pb- and Cu-hydrosulfide complexes predominant over chloride complexes at medium to high temperature fluids that saturated in Fe-S sulfides (Zhong et al., 2015a). An interesting result is that the epigenetic ore-fluid has greater ability in transporting Cu than Zn and Pb (Fig. 11), because Cu (soft Lewis acid; Pearson, 1963) forms stronger bonds with reduced sulfur (soft Lewis base) than Zn and Pb (borderline Lewis acids). The greater mobility of Cu than Zn and Pb during metamorphism is cross-validated by both field observation (Gu et al., 2007) and geochemical experiments (Gu et al., 2004). This may account for the anomaly enrichment of Cu in the SEDEX ore-forming system (see Section 7.2).

## 6.2. The flow-through modeling

In the previous section, the chemical composition of initial ore-fluid is modeled at 300–400 °C. In this part, the initial ore-fluid at 350 °C flows through different lithological units while cooling (Fig. 12), to exam the lithological controls on sulfide precipitation. The lithological units that used in the flow-through modeling are designed to simulate the sequences of ore-hosting rocks (cf. Figs. 4 and 12).

The simulation indicates that a large volume of pyrrhotite (and minor pyrite) precipitates when the fluid encounters the interlayered Fe-rich carbonate (siderite), due to the interaction between Fe in the host rock and aqueous reduced sulfur, i.e., host rock sulfidation (Fig. 12). As a result, the content of reduced sulfur in the fluid declines dramatically, which will in turn destabilize metal-hydrosulfide complexes in the fluid and result in deposition of significant amounts of chalcopyrite, sphalerite, and to a lesser extent galena (Fig. 12). This agrees well the observation that high-grade Cu and Zn mineralization was formed by replacing siderite-magnesite host rocks along grain boundaries, and accompanying deposition of large amounts of pyrrhotite or pyrrhotite-pyrite assemblage (Fig. 7C–H; Zhong et al., 2015a,b). This mechanism controlled redistribution of sulfides during syntectonic and syntectonic metamorphic remobilization.

## 7. Discussion and conclusions

### 7.1. The multistage mineralization

The Dongshengmiao is a SEDEX-type deposit and underwent significant Zn, Pb and Cu remobilization during metamorphism and shear deformation. The syngenetic mineralization is manifested by the following facts: (1) The ore-hosting rift sequences is mainly composed of metamorphosed carbonaceous shale, dolomite, and clastic sediments, which are typical of SEDEX-type deposit. Intercalated metavolcanic rocks at the bottom of the ore-hosting sequences indicate an abnormally high geothermal gradient, which would favor the development submarine hydrothermal systems (Peng and Zhai, 1997). Furthermore, B-, Mn-, P-, Ba-enriched layers and siderite layers within the ore-hosting sequences are indicators of submarine hydrothermal activity (Zhai et al., 2008; Zhang et al., 2010). (2) In the northeast region of the deposit, where shear deformation was relatively weak, the orebodies are generally stratabound and stratiform (Figs. 3 and 5). (3) The pre-tectonic fine-

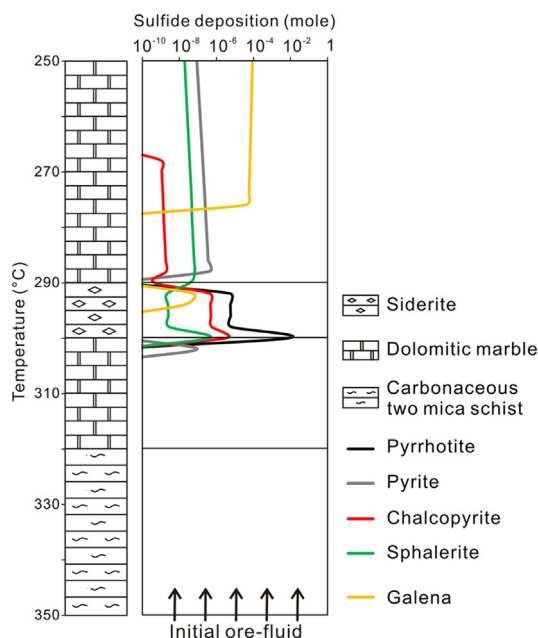


**Figure 12.** The result of the flow-through thermodynamic modeling, showing the amounts of sulfide precipitation as a result of fluid-rock interaction and fluid cooling (right). Also shown is the lithology of the rock sequences designed for the modeling (left). The modeling is carried out at a temperature increment of 5 °C for each step, and the pressure is fixed at 2.5 kbar.

grained massive pyrite is an index of submarine exhalative mineralization (Fig. 6). Relics of marcasite cores are locally preserved in fine-grained pyrite, suggesting that it was originally formed under a low-temperature syngenetic condition. (4) Sulfides except for chalcopyrite are strongly enriched in heavy sulfur isotopes (Fig. 9), suggesting that they were originally deposited in a submarine exhalative ore-forming system by reduction of marine sulfate. Sulfides are depleted in radiogenic lead and have Proterozoic two-stage lead model ages (Fig. 8), indicating that Pb was firstly enriched as stratabound sulfides accompanying development of the ore-hosting rift rocks.

During the early Cretaceous orogeny, large-scale Zn-Pb-Cu remobilization took place as a result of metamorphism and accompanying shear deformation, with the assist of metamorphic fluid. Zn-Pb-Cu sulfides and accompanying hydrothermal gangue minerals occurs filling shear structures of mylonitic host rocks (Fig. 7A, B), or replacing chemically active Fe-rich carbonates (Fig. 7C–H).

The metamorphic process resulted in recrystallization of massive pyrite, modification of the oxygen and hydrogen systematics, and most importantly, redistribution of economic sulfides. Redistribution of Zn-Pb-Cu sulfides is controlled by both structures and host rock geochemistry. Orebodies in the southwest region of the deposit are strongly controlled by the thrusts. They are consistently northwest-dipping and share similar dip angles with the thrust faults, and asymmetrically folded due to the activity of the thrusts (Fig. 5). The orebodies were upgraded at hinge regions of the folds (Chen and Peng, 2008), indicating the redistribution of ore-forming elements during deformation. During the remobilization, Zn-Pb-Cu would be preferentially redistributed into Fe-rich carbonates, for they are ideal sites for reprecipitation of sulfides (Fig. 12; Zhong et al., 2015b). The lithological control during sulfide redistribution can partly account for the stratiform nature of the orebodies, for high-grade replacement mineralization is expected to extend along siderite-rich layers of the host rock sequences.

## 7.2. A preliminary interpretation on the unusual enrichment of Cu

Most SEDEX deposits are characterized by large tonnages of Zn and Pb, with Zn reserves several times higher than Pb. They averagely have a Zn/(Zn + Pb) ratio of 0.7 (Leach et al., 2005; Table 4). Similarly, our previous thermodynamic simulation on the chemical composition of a SEDEX ore-fluid yielded Zn/(Zn + Pb) ratios ranging from 0.86 to 0.90 (Zhong et al., 2015a; Table 4). On the contrary, Cu is subeconomic in most SEDEX deposits, with a few Cu-rich exceptions having Cu/(Zn + Pb) ratios up to ~0.05 (e.g., Mt. Isa; Leach et al., 2005; Pirajno, 2009). Previous thermodynamic simulation (Zhong et al., 2015a) also reveals a very low solubility of Cu in the SEDEX ore-forming fluids (Cu/(Zn + Pb) < 0.0005; Table 4). In the case of Cu-rich Mt. Isa deposit, most researchers interpreted the enrichment of Cu as a result of epigenetic hydrothermal overprinting on syngenetic Zn-Pb-Ag orebodies during metamorphism and deformation (Large et al., 2005).

In the case of the Dongshengmiao, its Zn and Pb tonnages agree well with typical SEDEX deposits in the world, with a Zn/(Zn + Pb) ratio of 0.83 (Table 4), consistent with the conclusion that Zn and Pb were originally enriched in a submarine exhalative ore-forming system. In addition, the enrichment of about 11.9 g/t Ag accompanying Zn and Pb at the Dongshengmiao is also characteristic of SEDEX ore-forming systems (Leach et al., 2005).

The Dongshengmiao has an unusually greater Cu endowment than most SEDEX deposits. It has a Cu/(Zn + Pb) tonnage ratio of 0.019, about two orders of magnitude higher than the thermodynamic prediction (Table 4). Here we propose a preliminary hypothesis that the enrichment of Cu is a result of synmetamorphic hydrothermal activity. The thermodynamic modeling (Section 6.1) indicates that the ore-fluid during sulfide remobilization has a great potential in transporting Cu due to its high temperature and high content of reduced S (Fig. 11). The thermodynamic modeling predicts that the Cu/(Zn + Pb) ratio in the ore-fluid is as high as 6.5 (Table 4). The high solubility of Cu in the metamorphic ore-fluid enables the fluid to strip a large amount of Cu from the fluid source during devolatilization, i.e., Cu was extracted from “normal” sources without pre-enrichment. On the contrary, the relatively low solubility of Zn and Pb excludes the possibility that they were sourced from normal crustal rocks together with Cu. To form this giant Zn-Pb deposit, the syngenetic enrichment of Zn and Pb seems to be a necessity, because the epigenetic fluid is not capable to transport such a large volume of ore-forming elements. Therefore, the metamorphic fluid played a dual role in ore formation. First, when the fluid infiltrated the syngenetic sulfides during metamorphism, it provided a medium that would enhance the *in situ* remobilization and recrystallization of sulfides, for example by the fluid-assisted diffusive or advective mass transfer (Marshall et al., 2000). Second, the metamorphic fluid can scavenge Cu from a large volume of source rocks during devolatilization, and precipitate it when infiltrating syngenetic Zn-Pb orebodies. This hypothesis is evidenced by the sulfur isotopic signatures of sulfides. The markedly lighter sulfur isotopes of chalcopyrite suggest that the Cu had a different source from sphalerite and galena (Fig. 9). Furthermore, Cu mineralization took place mostly in the southwest region of the deposit where thrust faults were widely developed. Contrarily, it is generally subeconomic in the northeast region, where shear deformation was much weaker. This is consistent with the hypothesis that Cu mineralization was a result of syntectonic hydrothermal overprinting.

## 8. Conclusion: the genetic model

During Proterozoic, syngenetic SEDEX-type mineralization took place during the development of a rift, forming stratabound massive pyrite, Zn-Pb sulfides, and siderite-rich layers. In early Cretaceous, the rift sequences underwent lower greenschist facies metamorphism and shear deformation, as a result of Yanshanian orogeny and thrusting. Stratabound Zn-Pb sulfides were remobilized with the assistance of metamorphic fluids, and redistributed under the controls of thrust faults and host rock lithology. After a short distance of liquid state remobilization, Zn-Pb sulfides were

**Table 4**

Metal ratios of the Dongshengmiao deposit, in comparison with typical SEDEX deposits and the ore-fluid during synmetamorphic remobilization.

	Tonnage of the Dongshengmiao	Ore-fluids of SEDEX deposits <sup>a</sup>	Tonnages of SEDEX deposits <sup>b</sup>	Fluid of remobilization <sup>c</sup>
Zn/(Zn + Pb)	0.83	0.86–0.90	~0.7 in average	0.28
Cu/(Zn + Pb)	0.019	0.00028–0.00043	Mostly subeconomic	6.5

<sup>a</sup> Based on the thermodynamic modeling by Zhong et al. (2015a).

<sup>b</sup> Based on the compilation of tonnages of SEDEX deposits provided by Leach et al. (2005).

<sup>c</sup> Based on the simulation of Section 6.1.

re-deposited in shear structures, forming the shear-zone controlled mineralization that similar with orogenic-type deposits. In addition, siderite-rich layers within the host rock sequences are ideal traps for sulfide reprecipitation, and therefore hosting high-grade replacement mineralization. The metamorphic fluid not only played a role as a medium that facilitated the short-distant remobilization and redistribution of Zn-Pb sulfides, but also striped a large amount of Cu from the fluid source during devolatilization. The Cu-mineralized metamorphic fluid infiltrated and dissolved the syngenetic Zn-Pb sulfides, and eventually deposited Cu-rich orebodies accompanying the remobilized Zn and Pb sulfides.

The Dongshengmiao provides a case of an SEDEX ore-forming system overprinted by an orogenic-type mineralization/remobilization event. In a perspective of tectonic settings, the former is a typical case of mineralization that formed in extensional settings such as rifts, while the latter indicates a compressional setting, i.e., orogenic belt. The North China Block is a very unique case of Archean craton that was reactivated during Mesozoic. It provides unusual tectonic settings for the genesis of large-scale remobilized SEDEX deposit that has hybrid geological and geochemical characteristics of both SEDEX and orogenic-type deposits, and unusual enrichment of Cu as a SEDEX deposit.

## Acknowledgments

This paper was completed under the instruction of Prof. Yanjing Chen. This study was financially supported by the National Basic Research Program of the People's Republic of China (Nos. 2013CB429801, 2006CB403500), the National Natural Science Foundation of China (Nos. 40972057, 41502069), and the Post-doctoral Science Foundation of China (No. 2015M570033). We gratefully acknowledge the Zijin Mining Group Co. Ltd and Drs. Yongfei Yang and Chuansheng Hu for their help during fieldwork. Prof. Yuling Xie is thanked for offering us practical guide on petrographic observation.

## References

- Brueckner, S.M., Piercey, S.J., Sylvester, P.J., Maloney, S., Pilgrim, L., 2014. Evidence for syngenetic Precious metal enrichment in an Appalachian volcanogenic massive sulfide system: the 1806 zone, ming mine, Newfoundland, Canada. *Economic Geology* 109, 1611–1642.
- Chen, B., Jahn, B.M., Tian, W., 2009a. Evolution of the Solonker suture zone: constraints from zircon U–Pb ages, Hf isotopic ratios and whole-rock Nd–Sr isotope compositions of subduction- and collision-related magmas and fore-arc sediments. *Journal of Asian Earth Sciences* 34, 245–257.
- Chen, G.H., 1990. A study on the material source of the Dongshengmiao polymetallic sulfide deposits Inner Mongolia. *Journal of Hebei College of Geology* 13, 364–374 (in Chinese with English abstract).
- Chen, X.F., Peng, R.M., 2008. Analysis on the geological structural factors leading to the Dongshengmiao super-large deposit. *Contributions to Geology and Mineral Resources Research* 23, 182–186 (in Chinese with English abstract).
- Chen, Y.J., 2002. Several problems in study of regional metallogenesis in China: their relationship to continental collision. *Earth Science Frontiers* 9, 319–328 (in Chinese with English abstract).
- Chen, Y.J., 2006. Orogenic-type deposits and their metallogenic model and exploration potential. *Geology in China* 33, 1181–1196 (in Chinese with English abstract).
- Chen, Y.J., Chen, H.Y., Zaw, K., Pirajno, F., Zhang, Z.J., 2007a. Geodynamic settings and tectonic model of skarn gold deposits in China: an overview. *Ore Geology Reviews* 31, 139–169.
- Chen, Y.J., Ni, P., Fan, H.R., Pirajno, F., Lai, Y., Su, W.C., Zhang, H., 2007b. Diagnostic fluid inclusions of different types hydrothermal gold deposits. *Acta Petrologica Sinica* 23, 2085–2108 (in Chinese with English abstract).
- Chen, Y.J., Zhai, M.G., Jiang, S.Y., 2009b. Significant achievements and open issues in study of orogenesis and metallogenesis surrounding the North China continent. *Acta Petrologica Sinica* 25, 2695–2726 (in Chinese with English abstract).
- Chen, Y.J., Zhang, C., Li, N., Yang, Y.F., Deng, K., 2012. Geology of the Mo deposits in Northeast China. *Journal of Jilin University (Earth Science Edition)* 42, 1223–1268 (in Chinese with English abstract).
- Clayton, R.N., O'Neil, J.R., Mayeda, T.K., 1972. Oxygen isotope exchange between quartz and water. *Journal of Geophysical Research* B77, 3057–3067.
- Darby, B.J., Ritts, B.D., 2007. Mesozoic structural architecture of the Lang Shan, North-Central China: intraplate contraction, extension, and synorogenic sedimentation. *Journal of Structural Geology* 29, 2006–2016.
- Ding, T.P., Jiang, S.Y., 2000. Stable isotope study of the Langshan polymetallic mineral district, Inner Mongolia, China. *Resource Geology* 50, 25–38.
- Dong, S.W., Zhang, Y.Q., Chen, X.H., Long, C.X., Wang, T., Yang, Z.Y., Hu, J.M., 2008. The formation and Deformational characteristics of east Asia multi-direction convergent tectonic system in late Jurassic. *Acta Geoscientica Sinica* 29, 306–317 (in Chinese with English abstract).
- Gao, Z.F., Zhu, X.K., Luo, Z.H., Sun, J., Zhang, F.F., Gao, W.G., Wang, B.L., Zhong, C.H., 2014. Geological and geochemical characteristics of the main ore-bearing rock series in the Dongshengmiao superlarge polymetallic sulfide deposit and their implications for ore genesis. *Acta Petrologica et Mineralogica* 33, 825–840 (in Chinese with English abstract).
- Goldfarb, R.J., Baker, T., Dube, B., Groves, D.L., Hart, C.J.R., Gosselin, P., 2005. Distribution, character, and genesis of gold deposits in metamorphic terranes. *Economic Geology* 100th Anniversary Volume, pp. 407–475.
- Goldfarb, R.J., Newberry, R.J., Pickthorn, W.J., Gent, C.A., 1991. Oxygen, hydrogen, and sulfur isotope studies in the Juneau gold belt, Southeastern Alaska: constraints on the origin of hydrothermal fluids. *Economic Geology* 86, 66–80.
- Gong, W.B., 2014. Characteristics and significances of structural deformation of western part of the North China Craton in the late Paleoproterozoic. *Chinese Academy of Geological Sciences, Beijing*, 174 pp.
- Gu, L.X., Tang, X.Q., Wang, Z.J., Sun, Y., Wu, C.Z., Xiao, X.J., Ni, P., Wu, X.Y., 2004. Remobilisation experiment of chalcopyrite in massive sulphide ore by NaCl solution at 362 °C and a differential stress. *Lithos* 73 (1–2), S47.
- Gu, L.X., Zheng, Y.C., Tang, X.Q., Zaw, K., Della-Pasque, F., Wu, C.Z., Tian, Z.M., Lu, J.J., Ni, P., Li, X., Yang, F.T., Wang, X.W., 2007. Copper, gold and silver enrichment in ore mylonites within massive sulphide orebodies at Hongtoushan VHMS deposit, N.E. China. *Ore Geology Reviews* 30, 1–29.
- Hebei College of Geology and Geological Prospecting Team of Inner Mongolia Chemical Industry, 1980. Host rock sequences and structures of the Dongshengmiao pyritic deposit in Bayan Nur, Inner Mongolia. *Journal of Hebei College of Geology* 3, 47–66 (in Chinese).
- Hu, C.S., Li, W.B., Xu, C., Zhong, R.C., Zhu, F., Qiao, X.Y., 2015. Geochemistry and Petrogenesis of Permian Granitoids in the Northwestern Margin of the North China Craton: Insights from the Dongshengmiao Pluton, Inner Mongolia. *International Journal of Geology Review* 57 (14), 1843–1860.
- Hu, X., Gao, Q.W., Sun, G.Y., Lü, Y.F., 1981. A study on faults in the Dongshengmiao district, Bayannaer League, Inner Mongolia. *Journal of Shijiazhuang University of Economics* 4, 31–93 (in Chinese with English abstract).
- Huang, W.X., 2009. Research on the Mine-forming Character of Polymetallic Sulfide Deposits in Langshan District, Proterozoic. *Chengdu University of Technology, Chengdu*, p. 60 (in Chinese with English abstract).
- Jiang, X.Q., 1994. Some evidence for contemporaneous faults in the Dongshengmiao sulfide polymetallic ore district in Inner Mongolia and the genesis of the ore deposit. *Mineral Deposits* 13, 49–60 (in Chinese with English abstract).
- Large, R.R., Bull, S., McGoldrick, P.J., Waters, S., Derrick, G.M., Carr, G.R., 2005. Stratiform and Stratabound Zn–Pb–Ag Deposits in Proterozoic Sedimentary Basins, Northern Australia. *Economic Geology* 100th Anniversary Volume, pp. 931–963.
- Leach, D.L., Bradley, D.C., Huston, D., Pisarevsky, S.A., Taylor, R.D., Gardoll, S.J., 2010. Sediment-hosted lead-zinc deposits in earth history. *Economic Geology* 105, 593–625.
- Leach, D.L., Sangster, D.F., Kelley, K.D., Large, R.R., Garven, G., Allen, C.R., Gutzmer, J., Walters, S., 2005. Sediment-hosted Lead-Zinc Deposits: a Global Perspective. *Economic Geology* 100th Anniversary Volume, pp. 561–608.
- Li, Q.L., Chen, F.K., Guo, J.H., Li, X.H., Yang, Y.H., Siebel, W., 2007. Zircon ages and Nd–Hf isotopic composition of the Zhaertai Group (Inner Mongolia): evidence for early Proterozoic evolution of the northern North China Craton. *Journal of Asian Earth Sciences* 30, 573–590.
- Li, Z.L., Xu, W.D., Pang, W.Z., 1986. S, Pb, C and O isotopic compositions and ore genesis of the stratabound polymetallic sulfide deposits in middle Inner Mongolia, China. *Geochimica* 1, 13–22 (in Chinese with English abstract).
- Liu, Y., 2012. Geochemical and Chronological Characteristics of the Granitic Gneisses and Intrusive Rocks from Dongshengmiao Ore District, Inner Mongolia and their Tectonic Implications. M.S. thesis. Lanzhou University, Lanzhou (in Chinese with English abstract).
- Long, L.Z., 2009. Geological Characteristics and Genesis Analysis of Dongshengmiao Lead-Zinc Ore Deposit in the Inner Mongolia. M.S. thesis. Central South University (in Chinese with English abstract).
- Marignac, C., Diagona, B., Cathelineau, M., Boiron, M., Banks, D., Fourcade, S., Vallance, J., 2003. Remobilisation of base metals and gold by Variscan metamorphic fluids in the south Iberian pyrite belt: evidence from the Tharsis VMS deposit. *Chemical Geology* 194, 143–165.
- Marshall, B., Spry, P.G., 2000. Discriminating between regional metamorphic remobilization and syntectonic emplacement in the genesis of massive sulfide ores. *Reviews in Economic Geology* 11, 39–80.
- Marshall, B., Vokes, F.M., Laroque, A.C.L., 2000. Regional metamorphic remobilization: upgrading and formation of ore deposits. *Reviews in Economic Geology* 11, 19–38.
- Miu, Y.X., Ran, C.Y., 1992. Geological and geochemical characteristics of Dongshengmiao Pb–Zn–S deposit of submarine exhalative origin, Inner Mongolia. *Geochimica* 21, 375–382 (in Chinese with English abstract).

- Moura, A., 2008. Metallogeneses at the Neves Corvo VHMS deposit (Portugal): a contribution from the study of fluid inclusions. *Ore Geology Reviews* 34, 354–368.
- Niu, S.Y., Xu, C.S., Hu, X., Sun, A.Q., 1991. A study of ore-control structure in the Langshan Mountain area, Inner Mongolia. *Journal of Changchun University of Earth Science* 21, 313–320 (in Chinese with English abstract).
- Ohmoto, H., Rye, R., 1979. Isotopes of sulfur and carbon. In: Bernes, H.L. (Ed.), *Geochemistry of Hydrothermal Ore Deposits*, second ed. John Wiley and Sons, New York, pp. 509–567.
- Pearson, R.G., 1963. Hard and soft acids and bases. *Journal of the American Chemical Society* 85, 3533–3539.
- Peng, R.M., Zhai, Y.S., 1997. The confirmation of the metamorphic double-peaking volcanic rocks in Langshan Group of the Dongshengmiao ore district, Inner Mongolia and its significance. *Earth Science—Journal of China University of Geosciences* 22, 589–594 (in Chinese with English abstract).
- Peng, R.M., Zhai, Y.S., 2004. The characteristics of hydrothermal exhalative mineralization of the Langshan-Zhaertai belt, Inner Mongolia, China. *Earth Science Frontiers* 11, 257–264 (in Chinese with English abstract).
- Peng, R.M., Zhai, Y.S., Chen, X.F., Liu, Q., Lv, J.Y., Shi, Y.X., Wang, G., Li, S.B., Wang, L.G., Ma, Y.T., Zhang, P., 2010. Discovery of Neoproterozoic acid volcanic rock in the south-western section of Langshan, Inner Mongolia. *Chinese Science Bulletin* 55, 2611–2620 (in Chinese with English abstract).
- Peng, R.M., Zhai, Y.S., Han, X.F., Wang, J.P., Wang, Z.G., Qin, J.W., 2007a. Magmatic hydrothermal overprinting in the Mesoproterozoic Dongshengmiao deposit, Inner Mongolia: geological and fluid inclusion evidences. *Acta Petrologica Sinica* 23, 145–152.
- Peng, R.M., Zhai, Y.S., Han, X.F., Wang, Z.G., Wang, J.P., Shen, C.L., Chen, X.F., 2007b. Mineralization response to the structural evolution in the Langshan orogenic belt, Inner Mongolia. *Acta Petrologica Sinica* 23, 679–688 (in Chinese with English abstract).
- Peng, R.M., Zhai, Y.S., Wang, Z.G., 2000. Ore-controlling synchronous faults of Mesoproterozoic Dongshengmiao and Jiashengpan SEDEX-type ore deposits, Inner Mongolia. *Earth Science—Journal of China University of Geosciences* 4, 404–410 (in Chinese with English abstract).
- Pirajno, F., 2009. *Hydrothermal Processes and Mineral Systems*. Springer, Netherlands, p. 1250.
- Rui, Z.Y., Shi, L.D., Fang, R.H., 1994. *Geology of Nonferrous Metallic Deposits in the Northern Margin of the North China Landmass and its Adjacent Area*. Geological Publishing House, Beijing (in Chinese with English abstract).
- Sengör, A.M.C., Natal'in, B.A., 1996. *Paleotectonics of Asia: Fragments of Synthesis and the Tectonic Evolution of Asia*. Cambridge University Press, Cambridge, pp. 486–640.
- Shvarov, Y., Bastrakov, E., 1999. HCh: a Software Package for Geochemical Equilibrium Modelling. User's Guide Record/25. Australian Geological Survey Organisation, Canberra.
- Sheppard, S., 1986. Characterization and isotopic variations in natural waters. *Mineralogy* 16, 165–183.
- Stacey, J.S., Kramers, J.D., 1975. Approximation of terrestrial lead isotope evolution by a two-stage model. *Earth and Planetary Science Letters* 26, 207–221.
- Sun, A.Q., Niu, S.Y., 1994. Structure control on mineralization and prognosis in the Dongshengmiao troilite mine. *Geological Exploration for Non-Ferrous Metals* 3, 146–150 (in Chinese with English abstract).
- Sun, W.D., Ding, X., Hu, Y.H., Li, X.H., 2007. The golden transformation of the cretaceous plate subduction in the west Pacific. *Earth and Planetary Science Letters* 262, 533–542.
- Suo, W., 1992. Characteristics and genesis of thrust faults in the Dongshengmiao mining area, Inner Mongolia. *Geology of Chemical Minerals* 14, 50.
- Suzuoki, T., Epstein, S., 1976. Hydrogen isotope fractionation between OH-bearing minerals and water. *Geochimica et Cosmochimica Acta* 40, 1229–1240.
- Taylor, H.P., 1974. The application of oxygen and hydrogen isotope studies to problems of hydrothermal alteration and ore deposition. *Economic Geology* 69, 843–883.
- Tornos, F., 2006. Environment of formation and styles of volcanogenic massive sulfides: the Iberian Pyrite Belt. *Ore Geology Reviews* 28, 259–307.
- Wang, C., Deng, J., Carranza, E.J.M., Lai, X., 2014. Nature, diversity and temporal-spatial distributions of sediment-hosted Pb–Zn deposits in China. *Ore Geology Reviews* 56, 327–351.
- Wulatehouqi Zijin Mining Group Co. Ltd, 2008. Report of Exploration on the Sanguiou South Ore Belt of the Dongshengmiao Deposit, Wulatehouqi, Inner Mongolia (in Chinese).
- Xia, X.H., 1992. Ore-forming characteristics and genetic discussion of the Dongshengmiao polymetallic pyrite deposits in Langshan metallogenic belt, Inner Mongolia. *Mineral Deposits* 11, 374–383 (in Chinese with English abstract).
- Xiao, W.J., Windley, B.F., Hao, J., Zhai, M.G., 2003. Accretion leading to collision and the Permian Solonker suture, Inner Mongolia, China: termination of the central Asian orogenic belt. *Tectonics* 22, 1069–1089.
- Xu, B., Charvet, J., Chen, Y., Zhao, P., Shi, G.Z., 2013. Middle Paleozoic convergent orogenic belts in western Inner Mongolia (China): framework, kinematics, geochronology and implications for tectonic evolution of the Central Asian Orogenic Belt. *Gondwana Research* 23, 1342–1364.
- Xu, J.H., Hart, C.J.R., Wang, L.L., Chu, H.X., Lin, L.H., Wei, X.F., 2011. Carbonic fluid overprints in volcanogenic massive sulfide deposits: examples from the Kelan volcanosedimentary basin, Altaides, China. *Economic Geology* 106, 145–155.
- Yakubchuk, A., 2004. Architecture and mineral deposit settings of the Altai orogenic collage: a revised model. *Journal of Asian Earth Sciences* 23, 761–779.
- Yang, J.P., 1992. The origin and the ore fabric property of the bedded lead–zinc (copper) sulfide deposit in Dong Sheng Miao, Inner Mongolia. *Journal of Hebei College of Geology* 5, 489–552 (in Chinese with English abstract).
- Zhai, Y.S., Peng, R.M., Chen, C.X., Cai, K.Q., Deng, J., Chen, X.M., Cheng, X.J., Wang, J.P., 2008. *Genesis and Structure of Major Metallogenic Series of China*. Geological Publishing House, Beijing (in Chinese with English abstract).
- Zhang, S.H., Zhao, Y., Song, B., Hu, J.M., Liu, S.W., Yang, Y.H., Chen, F.K., Liu, X.M., Liu, J., 2009. Contrasting late carboniferous and late permian–middle triassic intrusive suites from the northern margin of the North China craton: geochronology, petrogenesis, and tectonic implications. *Geological Society of America Bulletin* 121, 181–200.
- Zhang, Z.B., Li, J.H., Huang, C.Y., Liu, H., Zhao, Y.H., 2010. Study on genesis and ore prospecting of Dongshengmiao deposit in Inner Mongolia. *Journal of Jilin University (Earth Science Edition)* 40, 791–800 (in Chinese with English abstract).
- Zheng, Y., 2013. Metallogeny Related to the Permian–Triassic Orogenism in the CAOB—examples from 4 Polymetallic Deposits at the Southern Altay Orogen. The University of Chinese Academy of Sciences, Guangzhou, p. 242 (in Chinese with English abstract).
- Zheng, Y., Zhang, L., Chen, Y.J., Pete, H., Chen, H.Y., 2013. Metamorphosed Pb–Zn–(Ag) ores of the Keketale VMS deposit, Xinjiang: evidence from ore textures, fluid inclusions, geochronology and pyrite compositions. *Ore Geology Reviews* 54, 167–180.
- Zheng, Y.F., 1993. Calculation of oxygen isotope fractionation in hydroxyl-bearing silicates. *Earth and Planetary Science Letters* 120, 247–263.
- Zhong, R.C., Brugger, J., Chen, Y.J., Li, W.B., 2015a. Contrasting regimes of Cu, Zn and Pb transport in ore-forming hydrothermal fluids. *Chemical Geology* 395, 154–164.
- Zhong, R.C., Li, W.B., Chen, Y.J., Huo, H.L., 2012. Ore-forming conditions and genesis of the Huoqi Cu–Pb–Zn–Fe deposit in the northern margin of the North China craton: evidence from ore petrologic characteristics. *Ore Geology Reviews* 44, 107–120.
- Zhong, R.C., Li, W.B., Chen, Y.J., Ji, J.Q., Hu, C.S., Yang, Y.F., Hu, C., 2015b. Significant Zn–Pb–Cu remobilization of a syngenetic stratabound deposit during regional metamorphism: a case study in the giant Dongshengmiao deposit, northern China. *Ore Geology Reviews* 64, 89–102.
- Zhou, C.X., Zhang, Y.G., Tang, P.Z., Chen, Y.M., Wang, S.L., Qi, Y.H., Yang, Q., 2012. A discussion on genesis and ore prospecting of Dongshengmiao deposit, Inner Mongolia. *Journal of Jilin University (Earth Science Edition)* 42, 1656–1664 (in Chinese with English abstract).